MULTISTAGE AXIAL COMPRESSOR MAP GENERATION

Ágota KÓBOR

Department of Heat Engines
Technical University of Budapest
H-1521 Budapest, Hungary

Abstract

A one-dimensional theory regarding the change of state in a multistage axial compressor at design point and part load has been formulated. With regard to short calculation times for obtaining compressor maps this algorithm is suitable to get insight into the main parameters influencing the off-design behaviour. An 'academic' test example, representing a 3-stage subsonic compressor, has been used for tests.

Keywords: axial compressor, thermodynamic, computation method.

Introduction

In order to obtain a reliable operating map of a multistage axial compressor one has to perform comprehensive tests on a prototype machine or engage in computational work using detailed numerical programs with much empirical know-how. These requirements can be usually satisfied by compressor manufacturers only.

The objective of this work consists in calculating the operating map of compressors with satisfactory approximation by using relatively simple theories, combined with non-proprietary empirical data. The starting point of such work is the description of quasi one-dimensional flow along the mean diameter of the compressor channel (so-called pitchline theory) for each stage. Beginning with the specified inlet conditions to the first stage and a selected mass flow rate and proceeding to the second, third, etc. stages (stage stacking) one obtains the flow conditions at the compressor outlet and thus the operating point in the compressor map. By repeating the calculation for other conditions (e.g. other mass flow rates) and other shaft speeds the speed lines in the compressor map are obtained.

In addition to the specification of compressor geometry, empirical data are required about each blade row. Realistic results are only obtained if the row exit angle, and more importantly, the row losses are described as

functions of the flow conditions existing at the inlet to the blade row. Such functions can be provided on the basis of data published in the literature.

Symbols used:

a	[J/kg]	specific work	A	[m^2]	area
c	[m]	chord length	c	[m/s]	absolute velocity
c_s	[m/s]	speed of sound	D	[m]	diameter
DF	[-]	Liebleins diffusion factor	h	[J/kg]	specific enthalpy
l	[m]	blade length	M	[-]	Mach number
n	[-]	polytropic exponent	n	[l/s]	rotor speed
p	[Pa]	pressure	r	[-]	degree of reaction
R	[J/kg/K]	gas constant	T	[K]	temperature
u	[m/s]	blade speed	w	[m/s]	relative velocity
y	[J/kg]	spec. aerodyn. work			
α	[-]	absolute flow angle	β	[-]	relative flow angle.
γ	[–]	stagger angle	δ	[–]	clearence width
δh	[J/kg]	dissipation of energy	η	[–]	efficiency
φ	[-]	flow coefficient	κ	[-]	isentropic exponent
λ	[-]]	work coeff. of a stage	μ	[-]	mass flow coeff.
ν	[-]	blade speed coeff.	π	[-]	pressure ratio
θ	[-]	temperature ration	ρ	[kg/m^3]	density
ω	[-]	pressure loss coeff.	ψ	[-]	enthalpy coeff.
ζ	[-]	loss coefficient			

Subscripts

E	at the Euler radius	in	at the inlet
n	axial direction	N	at the hub
out	at the outlet	p	polytropic
P	profile	R	reference
S	at the tip	s	isentropic
SW	side-wall	TC	tip clearance
u	circumferential direction		
l	at rotor inlet	2	at rotor outlet
3	at stator outlet	0	at design point

Superscripts

o	total condition	-	overall compressor
"	rotor	'	stator
*	normalized with design point value		

For each stage we suppose:

  − the duct geometry and the rotor speed are known

- the inlet conditions (p_1, T_1, ρ_1) and the absolute inlet flow angle α_1 are known
- the cascade loss coefficient is affected by incidence angle and Mach number
- the rotor and stator exit angles are slightly variable with incidence angle
- the flow is subsonic in all stages.

With respect to the multistage configuration we suppose:

- the inlet conditions are given
- the flow angle to the first rotor is given by the inlet geometry
- all stages have a common shaft speed (single-spool compressor)
- the blading geometry is fixed (no adjustments provided).

We use the thermodynamic simplification:

- air is considered as a perfect gas.

Single-stage Theory

In order to understand the thermodynamic behaviour of a multistage axial flow compressor it is convenient to analyse only one stage at first. Using the one dimensional theory means that the flow phenomena are regarded in a single stream surface corresponding to the mean diameters given by the area averaged radius E (or 'Eulerian radius') at each station, i.e.

$$r_E = \sqrt{\frac{1}{2}(r_H^2 + r_T^2)} \ . \tag{1}$$

In the following the blade speed u at the Eulerian radius is of importance. Using the rotor speed n (revolutions per second) it can be calculated to

$$u = D_E \pi n = 2\pi r_E n \ . \tag{2}$$

Velocity Triangles

In order to compress the fluid in the stage it is necessary to raise the swirl component of the absolute velocity by the rotor row. Simultaneously the pressure increases because the relative flow decelerates. In the stator row the flow is deflected and the absolute velocity is reduced while the

pressure is rising further. The flow directions can be represented in velocity triangles (see *Fig. 1*, bottom). The triangles represent the absolute and relative velocities at rotor inlet, rotor outlet and stator outlet, always on the pertinent Eulerian mean radius (see *Fig. 1*, top, Planes 1,2,3). The absolute velocity c is related to the relative velocity w and the blade speed u by the following vector equation

$$\vec{c} = \vec{w} + \vec{u} \, . \tag{3}$$

The norm of the velocity vectors can be calculated as follows.

$$\left|\vec{c}\right| = \sqrt{c_n^2 + c_u^2} \, , \tag{4}$$

$$\left|\vec{w}\right| = \sqrt{w_n^2 + w_u^2} \, . \tag{5}$$

Introducing trigonometric functions the following equations are valid

$$\sin\alpha = \frac{c_n}{c} \, , \quad \cos\alpha = \frac{c_u}{c} \, , \quad \tan\alpha = \frac{c_n}{c_u} \, , \tag{6a}$$

$$\sin\beta = \frac{w_n}{w} \, , \quad \cos\beta = \frac{w_u}{w} \, , \quad \tan\beta = \frac{w_n}{w_u} \, , \tag{6b}$$

where α is the flow angle between the absolute velocity and the blade speed and β is the flow angle between the relative velocity and the blade speed. It is useful to introduce non-dimensional velocity relations. All velocities in the stage will be referred to the blade speed u_2 at rotor outlet,

$$C = \frac{c}{u_2} \, , \quad W = \frac{w}{u_2} \, , \quad U_1 = \frac{u_1}{u_2} \, , \quad U_2 = 1 \, . \tag{7}$$

Loading Limits

During compressor operation at lower mass flow rates the flow deceleration increases. Since the profile boundary layer of the suction side is not sufficiently supplied with kinetic energy the flow is separated and the stage reaches its stable operation limit (rotating stall). The limit of acceptable loading should not be exceeded in any compressor row. LIEBLEIN, see [5], defined a term, the diffusion factor

$$DF'' = 1\frac{w_2}{w_1}\frac{w_{u1} - w_{u2}}{2w_1}\left(\frac{t}{c}\right)'' \, , \tag{8}$$

$$DF' = 1\frac{c_3}{c_2}\frac{c_{u2} - c_{u3}}{2c_2}\left(\frac{t}{c}\right)' \, , \tag{9}$$

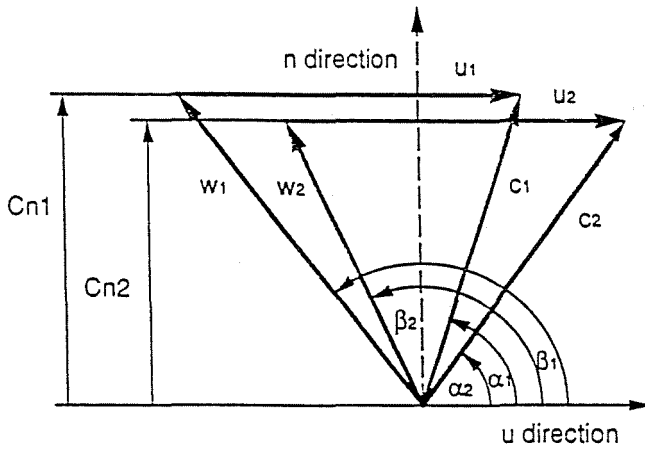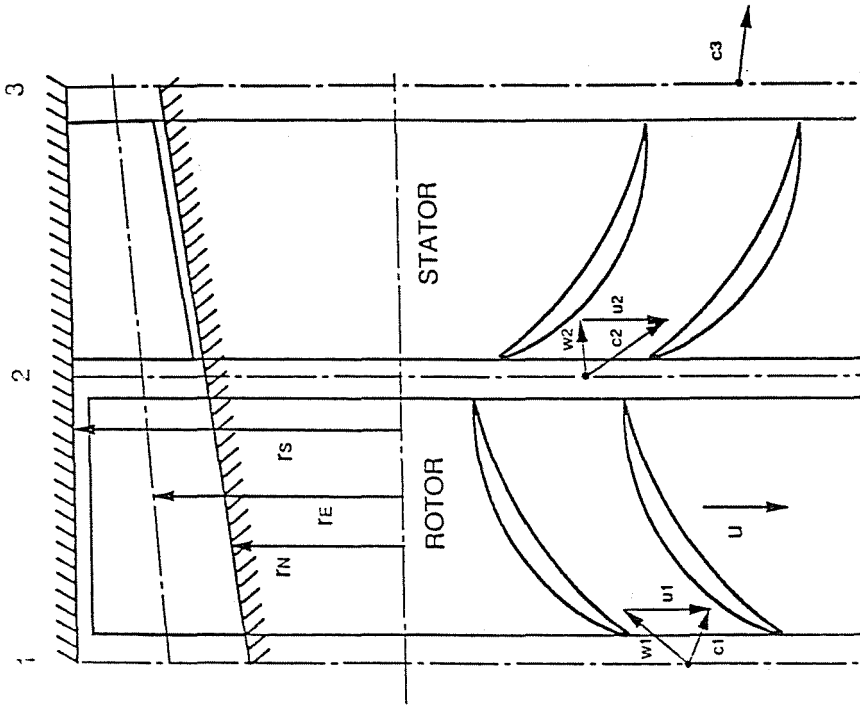which is limited to values of 0.4 to 0.6.

Fig. 1. Compressor stage and velocity triangles

Conservation Equations and Non-dimensional Coefficients

Generally it is convenient to express the data of any operating point by non-dimensional coefficients. Such coefficients are introduced for the through-flow velocity, the work transfer, the enthalpy rise (from which the pressure ratio can be obtained), the rotor speed and the mass flow rate.

The non-dimensional throughflow velocity $\frac{c_n}{u_2}$ is termed the flow coefficient

$$\varphi = \frac{c_n}{u_2} = C_{n2} \ . \tag{10}$$

For a compressor rotor row the energy equation can be written in the case of steady flow as follows

$$a = \left(h_2 + \frac{1}{2}c_2^2\right) - \left(h_1 + \frac{1}{2}c_1^2\right) = h_2^0 - h_1^0 \ . \tag{11}$$

In this equation a is the work supplied per unit mass of fluid and h represents the specific enthalpy. An adiabatic system is assumed. Considering the moment of momentum conservation the work can be expressed by Euler's equation

$$a = c_{u2}u_2 - c_{u1}u_1 \ . \tag{12}$$

Dividing by u_2^2 a non-dimensional number called the work coefficient of the stage is obtained

$$\lambda \equiv \frac{a}{u_2^2} = \frac{c_{u2}}{u_2} \frac{c_{u1}}{u_2} \frac{u_1}{u_2} \ . \tag{13}$$

Introducing trigonometric relations this leads to the following expression

$$\lambda = 1 - \varphi_2 \cot \beta_2 - \varphi_1 \frac{u_1}{u_2} \cot \alpha_1 \ . \tag{14}$$

If one regards the relative rotor exit angle β_2 and the absolute rotor inlet angle α_1 as constant, λ becomes a linear function of the φ. One can see that the work coefficient primarily depends on the flow coefficients and on blade row outlet angles. If the flow coefficients vary, e.g. due to a change of mass flow, the work coefficient will change, too.

The energy equation has the following form when applied to the stator, assuming adiabatic conditions:

$$h_3 + \frac{1}{2}c_3^2 = h_2 + \frac{1}{2}c_2^2 \ . \tag{15}$$

One can see that in the stator the total enthalpy $h^0 = h + c^2/2$ remains constant. In the non-dimensional form *Eq.* (15) is written as follows, with Ψ' called the stator enthalpy rise coefficient:

$$\Psi' \equiv \frac{h_3 - h_2}{u_2^2} = \frac{1}{2}(C_3^2 - C_2^2) \ . \tag{16}$$

The energy equation applied to the rotor had the form

$$a = \left(h_2 + \frac{1}{2}c_2^2\right) - \left(h_1 + \frac{1}{2}c_1^2\right) \ . \tag{17}$$

If the Eulerian equation is introduced, *Eq.* (15) leads to

$$h_2 + \frac{1}{2}w_2^2 - \frac{1}{2}u_2^2 = h_1 + \frac{1}{2}w_1^2 - \frac{1}{2}u_1^2 \ . \tag{18}$$

The left and right expressions are called rothalpy, a quantity which remains constant in the rotor. Dividing by u_2 one transfers the equation into the non-dimensional form, with Ψ'' called the rotor enthalpy rise coefficient:

$$\Psi'' \equiv \frac{h_2 - h_1}{u_2^2} = \frac{1}{2}(W_1^2 - W_2^2 - U_1^2 + 1) \ . \tag{19}$$

The pitchline rotor blade speed u_i at any control station $i = 1, 2, 3$ of the stage is made non-dimensional by the thermodynamic expression $\sqrt{c_p T}$ pertinent to the stage inlet stagnation conditions. The non-dimensional rotor blade speed thus obtained is

$$\nu = \frac{u}{\sqrt{c_p T_1^0}} \ . \tag{20}$$

The continuity equation is the third important conservation equation. To each cross-section i the mass flow is common:

$$m = \rho c_n A = \rho_i c_{ni} A_i \ , \tag{21}$$

where ρ is the density, c_n the axial velocity and A the annulus-sectional area. By dividing *Eq.*(21) by $A_1 \rho_1^0 \sqrt{c_p T_1^0}$ one can define a non-dimensional mass flow coefficient μ as

$$\mu \equiv \frac{m}{A_1 \rho_1^0 \sqrt{c_p T_1^0}} \ , \tag{22}$$

which has a common value for all three control stations of the stage. The non-dimensional mass flow coefficient is related to the flow coefficient φ, as seen from *Eqs.* (10), (21) and (22) by

$$\mu = \frac{A_i}{A_1} \frac{\rho_i}{\rho_i^0} \varphi_i \nu_i \ . \tag{23}$$

Finally, in order to characterise the compressor stage the so-called degree of reaction is defined

$$r = \frac{\Delta h''}{\Delta h'' + \Delta h'} = \frac{\Psi''}{\Psi'' + \Psi'} \ . \tag{24}$$

Compressors are usually designed with r of about 0.5 to 0.7. The static pressure rise in stages having $r = 0.5$ is equal in rotor and stator and the stage velocity triangles are symmetric.

The above equations link the energy transfer process (as expressed by enthalpies h and work a) and the density ρ to the fluid velocities. However, the interdependence of h and ρ is not yet formulated. This link is obtained by using the equations of state of the fluid and expressing the pressure rise in terms of velocity changes.

Thermodynamics

An isentropic change of fluid state is characterized by

$$\frac{p}{p_0} = \left(\frac{\rho}{\rho_0}\right)^\kappa, \quad \frac{T}{T_0} = \left(\frac{p}{p_0}\right)^{\frac{\kappa-1}{\kappa}} = \left(\frac{\rho}{\rho_0}\right)^{\kappa-1} \tag{25}$$

and

$$h - h_0 = c_p(T - T_0) = c_p T_0 \left[\left(\frac{p}{p_0}\right)^{\frac{\kappa-1}{\kappa}} - 1 \right] \ . \tag{26}$$

Real processes are non-isentropic, and it is convenient to describe them by a polytropic change in which the formalism of the isentrope is maintained, but a different exponent, the polytropic exponent n is used:

$$h - h_0 = c_p(T - T_0) = c_p T_0 \left[\left(\frac{p}{p_0}\right)^{\frac{n-1}{n}} - 1 \right] \ . \tag{27}$$

Polytropes are defined as processes during which the ratio $\nu dp/dh$ stays constant. For adiabatic compression processes the ratio is termed polytropic efficiency of the compression process:

$$\eta_p \equiv \frac{\nu dp}{dh} = \frac{dp}{\rho dh} \ . \tag{28}$$

The isentropic exponent κ and polytropic exponent n are linked by

$$\frac{n-1}{n} = \frac{1}{\eta_p}\frac{\kappa-1}{\kappa} \ . \tag{29}$$

Therefore the calculation of polytropic changes requires the knowledge of the polytropic efficiency η_p. This can be done on the basis of cascade and stage loss data.

Efficiency and Cascade Loss Computation Method

Prediction of Polytropic Efficiency

For any stage the adiabatic stage theory gives for the enthalpy rise the following equation

$$h_3 - h_1 = \Delta h'' + \Delta h' = \frac{1}{2}(w_1^2 - w_2^2 + u_2^2 - u_1^2) + \frac{1}{2}(c_2^2 - c_3^2) \ . \tag{30}$$

The polytropic law of the perfect gas gives the pressure rise in a stage as follows

$$\pi = \frac{p_3}{p_1} = \left[1 + \frac{h_3 - h_1}{c_p T_1}\right]^{\frac{n}{n-1}} \ , \tag{31}$$

where the polytropic exponent n follows from (29) if the stage polytropic efficiency η_p is known. The density rise in the stage follows as

$$\frac{\rho_3}{\rho_1} = \left(\frac{p_3}{p_1}\right)^{\frac{1}{n}} \ . \tag{32}$$

The objective of the stage loss calculation must be to predict the value of η_p on the basis of geometric data and flow conditions in the stage. For this purpose the behaviour of the rotor row and of the stator row have to be accounted for separately. The polytropic aerodynamic work νdp transferred to unit mass of fluid in the rotor row $(1 \rightarrow 2)$ and the stator row $(2 \rightarrow 3)$ are expressed in literature [1] by means of the row diffusion efficiencies hd for rotor and stator:

$$\int_1^2 \nu dp \equiv y'' = \eta_D'' \frac{w_1^2 - u_1^2 + u_2^2}{2} - \frac{w_2^2}{2} \ , \tag{33}$$

$$\int_2^3 \nu dp \equiv y' = \eta_D' \frac{c_2^2}{2} - \frac{c_3^2}{2} \ . \tag{34}$$

Here the polytropic aerodynamic work compressing the fluid is seen to be expressed as a fraction (η_D) of the kinetic energy at the inlet minus the entire kinetic energy at the outlet of the row. In rotating rows the kinetic energy is expressed with relative velocities and is enhanced by the contribution $(u_2^2 - u_1^2)/2$ of centrifugal forces. The factor η_D characterizes the loss of kinetic energy due to dissipation. Since the polytropic efficiency of the compressor stage $(1 \to 3)$ means

$$\eta_p \equiv \frac{\int_1^3 \nu dp}{h_3 - h_1} = \frac{y'' + y'}{\Delta h'' + \Delta h'} \tag{35}$$

one finds using *Eqs.* (30), (33) and (34)

$$1 - \eta_p = (1 - \eta_D'') \frac{w_1^2 - u_1^2 + u_2^2}{2(h_3 - h_1)} + (1 - \eta_D') \frac{c_2^2}{2(h_3 - h_1)} . \tag{36}$$

Thus, η_p can be obtained if η_D'' and η_D' are known.

Modelling of the Row Diffusion Losses

According to the literature on the analysis of compressor test data the diffusion efficiency η_D of any row (rotor or stator) can correlate with geometric and fluid dynamic parameters. Detailed correlations split up the total loss (energy dissipation) in the row into several parts. Following Traupel we write, by introducing a dissipation loss coefficient ζ for the contribution of blade profiles, side walls and tip clearance effects:

$$1 - \eta_D = \zeta_P + \zeta_{SW} + \zeta_{TC} . \tag{37}$$

For each of these loss coefficients a correlation can be given on the basis of experimental data obtained in cascade wind tunnels (for ζ_P) and in test compressors (for ζ_{SW} and ζ_{TC}).

Blade-profile Loss Coefficient
Conversion of Total Pressure Loss Data

Most cascade measurements published in technical literature express the blade profile loss simply in terms of a total pressure loss coefficient ω rather than in terms of a dissipation loss coefficient ζ_P. Therefore the values of

w must be transformed into ζ_P as shown below. The total pressure loss of any cascade is defined as

$$\omega = \frac{p_{in}^0 - p_{out}^0}{p_{in}^0 - p_{in}} \, , \qquad (38)$$

where index *in* and *out* refers to the conditions upstream and downstream of the cascade, respectively, and where all pressures are averages over the cascade annulus.

The total pressure loss is found to vary with the inlet Mach number

$$M_{in} = \frac{w_{in}}{\sqrt{\kappa R T_{in}}} \qquad (39)$$

and the inlet flow angle relative to the blades. The relative inlet velocity w_1 can be expressed in terms of total pressure as

$$\frac{w_{in}^2}{2} = c_p T_{in} \left[\left(\frac{p_{in}^0}{p_{in}} \right)^{\frac{\kappa-1}{\kappa}} - 1 \right] \, , \qquad (40)$$

from which, using (39)

$$\frac{p_{in}^0}{p_{in}} = \left[1 + \frac{\kappa-1}{2} M_{in}^2 \right]^{\frac{\kappa}{\kappa-1}} \, . \qquad (41)$$

The total pressure loss $p_{in}^0 - p_{out}^0$ is equivalent to a dissipation of kinetic energy δh given as

$$\delta h = c_p T_{in} \left[\left(\frac{p_{in}^0}{p_{in}} \right)^{\frac{\kappa-1}{\kappa}} - 1 \right] - c_p T_{in} \left[\left(\frac{p_{out}^0}{p_{in}} \right)^{\frac{\kappa-1}{\kappa}} - 1 \right] \, , \qquad (42)$$

$$\frac{\delta h}{c_p T_{in}} = \left(\frac{p_{in}^0}{p_{in}} \right)^{\frac{\kappa-1}{\kappa}} - \left(\frac{p_{out}^0}{p_{in}} \right)^{\frac{\kappa-1}{\kappa}} = \left(\frac{p_{in}^0}{p_{in}} \right)^{\frac{\kappa-1}{\kappa}} \left[1 - \left(\frac{p_{out}^0}{p_{in}} \right)^{\frac{\kappa-1}{\kappa}} \right] \, . \qquad (43)$$

The diffusion efficiency and the dissipation loss coefficient ζ_P refer the loss to the kinetic energy input to the row, cf. (33) and (34). This energy is given in the cascade experiment as $\frac{w_{in}^2}{2}$. Therefore we write for the cascade

$$\zeta_P = \frac{\delta h}{\frac{w_{in}^2}{2}} = \frac{1 + \frac{\kappa-1}{2} M_{in}^2}{\frac{\kappa-1}{2} M_{in}^2} \left[1 - \left(\frac{p_{out}^0}{p_{in}} \right)^{\frac{\kappa-1}{\kappa}} \right] \, , \qquad (44)$$

where 3(12) and the equivalence $\frac{w_{in}^2}{2} = c_p T_{in} \frac{\kappa - 1}{2} M_{in}^2$ have been used. Now (38) gives

$$\frac{p_{out}^0}{p_{in}^0} = \frac{p_{in}^0 - (p_{in}^0 - p_{in})\omega}{p_{in}^0} = 1 - \omega \left(1 - \frac{p_{in}}{p_{in}^0}\right) \tag{45}$$

and ζ_P can be expressed by w by inserting $Eq.$(38) into (45) and the latter into (44):

$$\zeta_P = \frac{1 + K}{K} \left\{ 1 - \left[1 - \omega \left(1 - [1 + K]^{\frac{\kappa}{\kappa - 1}} \right) \right]^{\frac{\kappa - 1}{\kappa}} \right\} , \tag{46}$$

where K is an abbreviation meaning

$$K \equiv \frac{\kappa - 1}{2} M_{in}^2 . \tag{47}$$

Equation (46) converts the total pressure loss coefficient w into a dissipation loss coefficient ζ_P. Experimental data on w obtained from cascades will therefore be used to express the profile loss ζ_P'' for rotor rows and ζ_P' for stator rows according to

$$\zeta_P'' = f(M_{w_1}, \beta_1) =$$
$$= \frac{1 + K''}{K''} \left\{ 1 - \left[1 - \omega''(M_{w_1}, \beta_1) \left(1 - [1 + K'']^{\frac{\kappa}{\kappa - 1}} \right) \right]^{\frac{\kappa - 1}{\kappa}} \right\} , \tag{48}$$
$$\zeta_P' = f(M_{c_2}, \alpha_2) =$$
$$= \frac{1 + K'}{K'} \left\{ 1 - \left[1 - \omega'(M_{c_2}, \alpha_2) \left(1 - [1 + K']^{\frac{\kappa}{\kappa - 1}} \right) \right]^{\frac{\kappa - 1}{\kappa}} \right\} . \tag{49}$$

If the cascade geometries of the two rows are different, the functional dependence of ω'' and ω' will be described by different experimental data.

Thus, an empirical function of the inlet angle and Mach number found by experiments with a particular cascade geometry can be transformed into an equivalent profile loss coefficient

$$\zeta_P'' = \zeta_P''(\beta_1, M_{w_1}) , \qquad \zeta_P' = \zeta_P'(\alpha_2, M_{c_2}) . \tag{50}$$

In low subsonic flow ($M_{w_1}, M_{c_2} \ll 1$), one finds $\zeta_P \approx \omega$. At higher Mach numbers, ζ_P tends to become slightly smaller than ω.

Determination of ω and Numerical Handling of Experimental Data

The basic problem of the blade pressure loss prediction in commercial compressors is the non-availability to the user of pertinent detailed proprietary

information. Unfortunately, however, only limited experimental material is published in the open literature. [Cumpsty, [5]].

An interesting set of detailed loss data referring to a subsonic compressor cascade was published by MAN'GHH [3]. The cascade profile loss was specified in function of inlet Mach number and inlet flow angle, *Fig. 2.* These detailed cascade loss curves will form the basis for testing the program on a 3-stage compressor configuration.
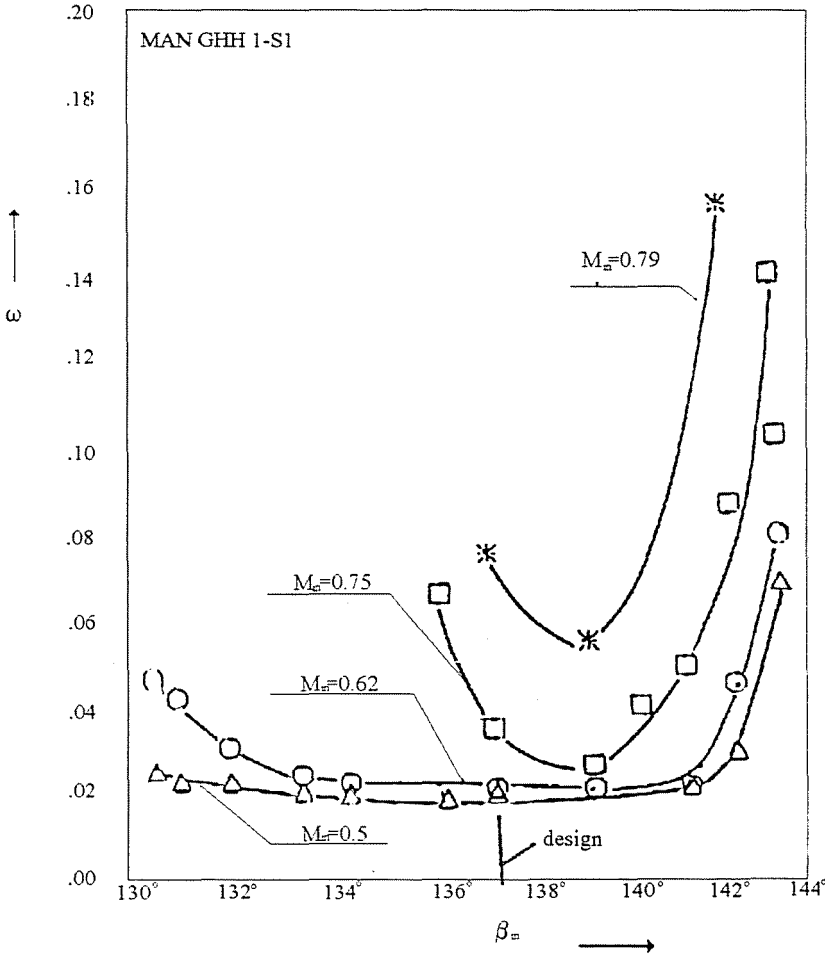

Fig. 2. Pressure loss coefficient versus inlet flow angle and Mach number

We note that
 - at low Mach number ($M_1 = 0.62$ and below) there is an inlet angle range where the profile loss is low (~ 0.02) and insensitive to β_1;

— at higher Mach number the range is narrowed and the loss increased;

— from $M_1 \sim 0.8$ upward the range of the cascade is reduced to almost zero and the losses increase dramatically.

These trends are typical for subsonic cascades with rounded leading edges.

The data of *Fig. 2* were obtained in a cascade wind tunnel. Such experimental loss data always refer to selected discrete values of inlet flow Mach number M_1 and inlet flow angle β_1. Interpolation both along M_1 and β_1 is therefore necessary during the use of w values for calculating a compressor map. (Note that subscripts 1 and 2 stand for 'in' and 'out', respectively.)

The present test results are limited to:

Mach number: $0.5 \ldots 0.79$ and

Incidence angle: $-7.0 \ldots +6.0$ deg (taking zero incidence at the design vale $\beta_{10} = 135$ deg)

This range is usually enough for our calculations, but to avoid an occasional run error in the program, the range was enlarged by reasonable extrapolation as shown in *Fig. 3*, to

Mach number: $0.25 \ldots 0.85$ and

Incidence angle: $-40.0 \ldots +40.0$ deg.

In order to get interpolated values from the diagram, a mesh was created with the experimental Mach numbers M_1 and with an array of β_1 coordinates. To increase the accuracy of the interpolation, the β_1 mesh was made dense in the most important area. The coordinates and the empirical function values at the points of intersection were stored in a data file. With the Mach number and incidence angle calculated by the program it is then possible to obtain sufficiently smooth cascade profile loss coefficient values from a simple linear interpolation subroutine.

Determination of Side-wall and Tip-clearance Losses

These loss data are typically of proprietary nature, and correlations published in literature are used as an estimate. Following Traupel we split up the rest losses of the row into side-wall and tip-clearance losses. In order to calculate the loss coefficients we use the following equations derived from empirical data published by several authors and summarized in [2]. Since these losses are produced near the casing and the rotor hub, they cannot be expressed on the basis of the pitchline conditions only.
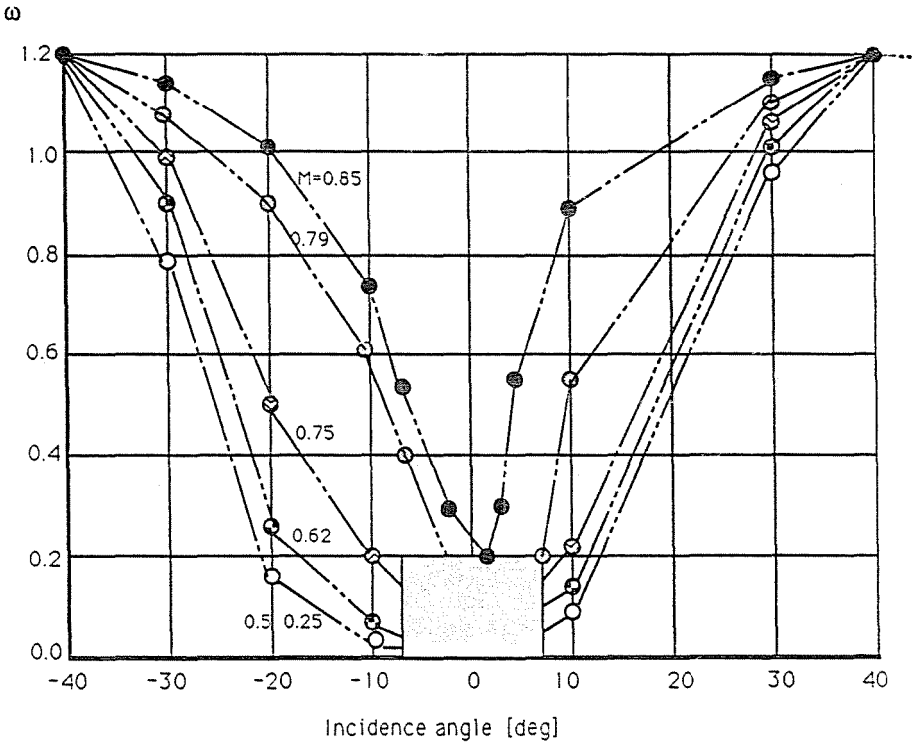
Fig. 3. Extrapolated ω values versus incidence angle and inlet Mach number

Rotor:

$$\zeta''_{SW} = c''_d \frac{\left(\frac{b}{l}\right)''}{\left(\frac{D_S}{D_N} + 1\right)\sin\beta_1}\left\{\left[\frac{w''_{\infty N}}{w_1}\right]^3 + \frac{D_S}{D_N}\left[\frac{c''_{\infty S}}{w_1}\right]^3\right\}\ , \qquad (51)$$

$$\zeta''_{TC} = K_0 \frac{\Delta W_{uS}}{\sin\gamma''_S}\left[\frac{w_{1S}}{w_1}\right]^2 \frac{D_S \delta''}{D_E l''}\ . \qquad (52)$$

Stator:

$$\zeta'_{SW} = c'_d \frac{\left(\frac{b}{l}\right)'}{\left(\frac{D_S}{D_N} + 1\right)\sin\alpha_1}\left\{\left[\frac{w'_{\infty N}}{c_2}\right]^3 + \frac{D_S}{D_N}\left[\frac{c'_{\infty S}}{c_2}\right]^3\right\}\ , \qquad (53)$$

$$\zeta'_{TC} = K_\delta \frac{\Delta C_{uN}}{\sin\gamma'_N}\left[\frac{c_{2N}}{c_2}\right]^2 \frac{D_N \delta'}{D_E l'}\ . \qquad (54)$$

Here the diameter ratios, DS/DN, b, δ and 1 are known from geometry and the velocities are known from the velocity triangles. The loss coefficient values c_d and $K\delta$ are taken from empirical diagrams presented by TRAUPEL [2].

Overview

The side-wall and tip-clearance losses together are typically of the same magnitude (2–3 %) as the profile loss ζ_P in its optimum range. Therefore the range of optimum compressor efficiency in a compressor map is determined mainly by the sensitivity of ζ_P to high positive or negative incidence angle values. All loss components taken together give a row diffusion efficiency η_D of the order of 94 to 96 % typically, resulting by way of $Eq.$ (36) in a stage polytropic efficiency η_P of about 0.88–0.92.

Multistage Compressor Pitchline Theory

Stage Stacking

The pitchline theory of a single compressor stage was introduced. All values of static and total temperature and pressure, velocities and enthalpy change of the rows were calculated along the main diameters. D_E of the compressor stage. As starting values it was necessary to specify the inlet conditions p_1 and T_1, the mass flow of working fluid and the absolute fluid flow angle α_1 at the inlet of the rotor. For all additional stages the procedure is repeated starting with the outlet conditions and the exit angle of the previous stage

$$p^0_{1,i+1} = p^0_{3,i}\,, \quad T^0_{1,i+1} = T^0_{3,i}\,, \quad \alpha_{1,i+1} = \alpha_{3,i}\,. \tag{55}$$

Inlet and Exit Casing

The fluid is led to the first blade row by an inlet casing. This inlet casing typically accelerates the flow 6 to 8 times and in subsonic compressors at design point the flow velocities in front of the first blade row range between $120 - 200$ m/s. The inlet casing has to ensure a regular circumferential distribution and a low loss inlet flow.

The exhaust diffusor leads the fluid to the exit flange or the outlet plenum, which may be the combustion chamber of gas turbines. The exit velocities of the last row are typically $150 - 250$ m/s. In order to recuperate this kinetic energy the exhaust duct is carefully shaped as a diffusor.

Since in the inlet and exit casing neither heat nor work transfer occur, the total energy is constant. Referring to TRAUPEL [1], the efficiency of a well shaped and highly accelerating inlet casing varies from $\eta_p = 0.9$ to 0.95. Its value is assumed to be known for the compressor considered.

The exit casing is shaped as a diffusor in order to recover pressure. Typical real values range from $c_p = 0.4$ to 0.6.

Calculation of Parameters Used in Compressor Map

Compressor maps express the relationship between shaft speed, flow rate, pressure ratio and efficiency over the entire useful operating range of the machine. They are usually presented in terms of non-dimensional numbers, in order to make the map transferable between members of a 'family' of geometrically similar compressors.

We will use normalized values of the non-dimensional coefficients, i.e. we will refer all values to the pertinent design-point value (subscript 0). In any operating point the rotor speed will be expressed by

$$\nu^* = \frac{\nu}{\nu_0} = \frac{n}{n_0}\sqrt{\frac{T_{in0}^0}{T_{in}^0}} \, , \tag{56}$$

the mass flow rate by

$$\mu^* = \frac{\mu}{\mu_0} = \frac{m}{m_0}\frac{\rho_{in0}^0}{\rho_{in}^0}\sqrt{\frac{T_{in0}^0}{T_{in}^o}} \, . \tag{57}$$

The overall pressure rise of the multistage compressor shall be expressed by the pressure rise coefficient

$$Y = \frac{\Pi - 1}{\Pi_0 - 1} = \frac{p_{in0}^0}{p_{in}^0}\frac{p_{out} - p_{in}^0}{p_{out0} - p_{in0}^0} \, , \tag{58}$$

where p_{out} is the static pressure at compressor outlet and p_{in}^0 is the total pressure at compressor inlet (subscript '0' stands for design point conditions). Note that Π_0 has very different values for different compressors (e.g. $\Pi_0 = 3$ for a single-stage centrifugal compressor and $\Pi_0 = 40$ for a turbojet compressor). The use of Y instead of Π/Π_0 makes the compressor maps look similar for very different values of Π_0 but conserves the linearity of the vertical scale with pressure ratio Π.

The overall polytropic efficiency of the compressor is defined by the sums $\overline{y}$ and $\overline{\Delta h}$ of stage aerodynamic work and stage enthalpy rise, respectively, as

$$\overline{\eta} \equiv \frac{\overline{y}}{\overline{\Delta h}} = \frac{\sum y_i}{\sum \Delta h_i} \, , \tag{59}$$

where the sum extends over the inlet, all stages 1 to z, and the outlet.
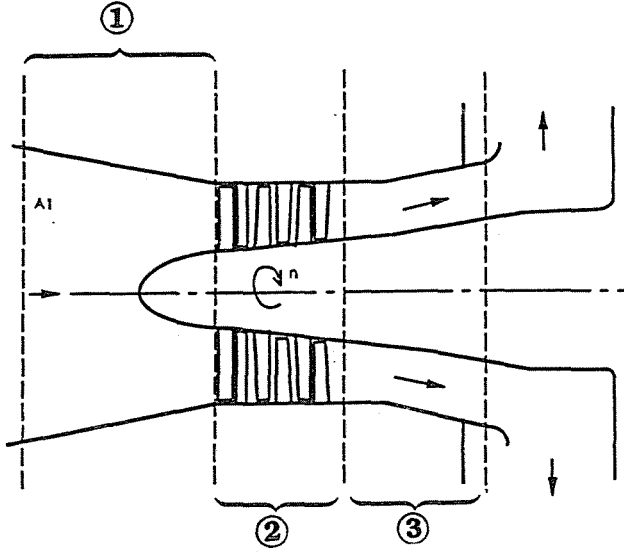
Compressor – calculation – input – data

general data		
66.	: massflow at compressor inlet at design-point	: [kg/s]
5000.	: number of revolutions at design-point	: [1/min]
1	: number of cascade-groups	: [–]
3	: number of stages	: [–]

inlet data		
2.00	: Al inlet area	: [m²]
0.95	: inlet efficiency	: [–]

diameters at compressor inlet (DN1, DS1)

0.497	: hub-diameter at compressor inlet	: [–]
0.900	: tip-diameter at compressor inlet	: [–]

1. stage: hub-diameter at rotor- and stator-outlet (DN2, DN3)

0.545	: 1. rotor outlet	: [–]
0.582	: 1. stator outlet	: [–]

2. stage: hub-diameter at rotor- and stator-outlet (DN2, DN3)

0.615	: 2. rotor outlet	: [–]
0.641	: 2. stator outlet	: [–]

3. stage: hub-diameter at rotor- and stator-outlet (DN2, DN3)

0.665	: 3. rotor outlet	: [–]
0.695	: 3. stator outlet	: [–]

1. stage: tip-diameter at rotor- and stator-outlet (DS2, DS3)

0.900	: 1. rotor outlet	: [–]
0.900	: 1. stator outlet	: [–]

2. stage: tip-diameter at rotor- and stator-outlet (DS2, DS3)

0.900	: 2. rotor outlet	: [–]
0.900	: 2. stator outlet	: [–]

3. stage: tip-diameter at rotor- and stator-outlet (DS2, DS3)

0.900	: 3. rotor outlet	: [–]
0.900	: 3. stator outlet	: [–]

1. group:

137.0	: bet1; inlet angle of relative flow at rotor inlet	: [grd]
110.0	: bet2; outlet angle of relative flow at rotor outlet	: [grd]
43.0	: alf2; outlet angle of absolute flow at rotor outlet	: [grd]
70.0	: alf3; outlet angle of absolute flow at rotor outlet	: [grd]
120.0	: gamrt; stagger angle rotor	: [grd]
120.0	: gamrt; stagger angle rotor	: [grd]
0.68	: ratio of circumfirential blade spacing / chord length (rotor)	
0.68	: ratio of circumfirential blade spacing / chord length (stator)	
0.30	: ratio of chord length / blade length (rotor)	: [−]
0.30	: ratio of chord length / blade length (stator)	: [−]
0.005	: delro; Clearence rotor	: [m]
0.004	: delst; Clearence stator	: [m]
3	: number of stages within this group	: [−]
MAN1	: rotor profile	: [−]
MAN1	: stator profile	: [−]

diffusor data
0.2	: area ratio	: [−]
0.7	: lamd	: [−]

③

Fig. 4. Compressor calculation input data

Test Case Results

As a first test case, we take the assumed data of a non-existing 'academic' 3-stage compressor including an inlet duct and an outlet diffusor. The data are shown in *Fig. 4*. With these data we have performed the compressor calculations for 5 different rotor speeds at ISO conditions. The curves shown in the following maps were calculated for steps in μ^* equalling 0.01.

The compressor map is shown in *Fig. 5*. The pressure ratio has a maximum and steeply falls off as mass flow μ^* is increased. It should be noted that the curves to the left of the maximum are unrealistic due to the occurrence of flow separation in one or more rows. The points where the diffusion criteria of Lieblein (or de Haller) are offended in any of the cascades are covered by a shaded area. The computer output (not seen here) shows that the front stage is becoming the critical one at low speed ν^* and the last stage at high speed.
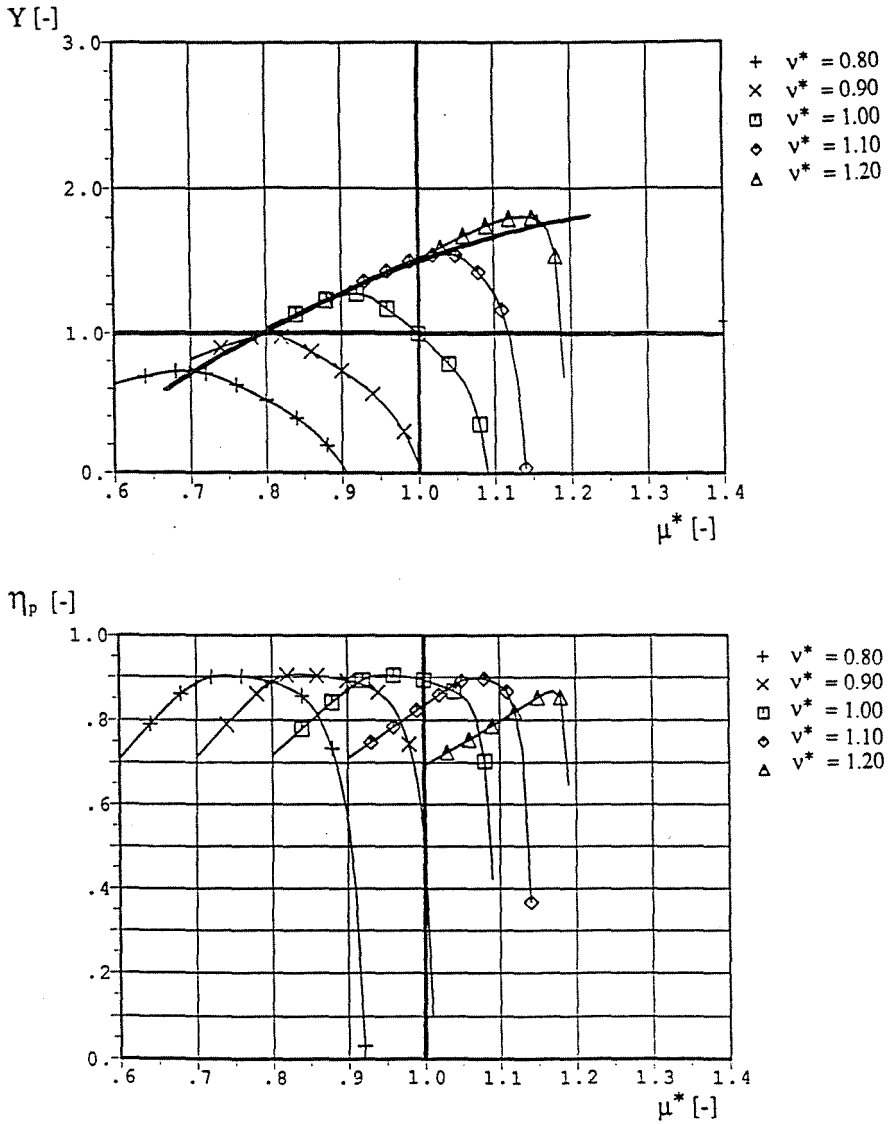
Fig. 5. Losses are dependent on incidence angle and Mach number. Pressure rise coefficient $Y = (\Pi - 1)/(\Pi_0 - 1)$ and polytropic efficiency $\eta_p = y/\Delta h$.

Conclusions

A one-dimensional theory regarding the change of state in a multistage axial compressor at design point and part load has been formulated. With regard to short calculation times for obtaining compressor maps this algorithm is suitable to get insight into the main parameters influencing the off-design behaviour. An 'academic' test example, representing a 3-stage subsonic compressor, has been used for tests.

A strong dependence of the cascade losses on flow incidence angle, taken from cascade wind tunnel experiments documented in the literature, produces close to realistic speed lines in the pressure vs. flow rate map and realistic compressor efficiency curves.

References

1. GYARMATHY, G. – ORTMANN, P. – KÓBOR, Á.: Axial Compressor Map Generation for Gas Turbine Process Calculations, Internal Report ETH Zürich 1993.
2. TRAUPEL, W.: Thermische Turbomaschinen, Parts I und II, Springer Verlag, Berlin, Heidelberg, 1988 und 1982.
3. W. STEINERT–B. EISENBERG–H. STARKEN: Design and Testing of a Controlled Diffusion Airfoil Cascade for Industrial Axial Flow Compressor Application, *ASME Journal of Turbomachinery*, Vol. 113 (1991) 10, pp. 583–590.
4. SEHRA ,A.– BETTNER, J.– COHN, A.: Design of a High Performance Axial Compressor for Utility Gas Turbine, *ASME Journal of Turbomachinery*, Vol. 114 (1992) 4, pp. 277–286.
5. CUMPSTY, N.A.: Compressor Aerodynamics, Longman Scientific and Technical, New York, 1989.